PHYSICAL REVIEW B VOLUME 59, NUMBER 10 1 MARCH 1999-II

# Direct evidence for filamentary and channel vortex flow in Pb/In superconducting films

M. Danckwerts, A. R. Goñi, and C. Thomsen
*Institut für Festkörperphysik, Technische Universität Berlin, Hardenbergstrasse 36, D-10623 Berlin, Germany*
(Received 24 August 1998)

Filamentary vortex flow in thin Pb/(14 at.%)In films is revealed by multiple voltage jumps in current-voltage ($IV$) characteristics below a critical magnetic field much lower than the upper critical field $B_{c2}$. The voltage jumps exhibit large counterclockwise hysteresis which diminishes with increasing field leading to bistable behavior close to the onset of free-flux flow. From the magnetic field and temperature dependence of the jump heights and currents at which jumps occur we infer that the number of flux lines in each channel or filament remains constant. In this regime, where the shear modulus of the vortex lattice is negligible, we find a nearly parabolic dependence of the depinning force on magnetic field, which is a signature of channel vortex motion. [S0163-1829(99)50710-8]

The vortex dynamics in type-II superconductors has received much attention partly due to its importance for the technological issue of superconductivity breakdown under a transport current, but also because its study has largely contributed to understanding disorder-driven effects on the vortex lattice. The influence of disorder potential on collective effects due to lattice pinning also plays a crucial role in related areas like Wigner-crystal formation in electron gases[1] and charge-density wave propagation.[2] In high-$T_c$ superconducting materials, phenomena such as vortex-lattice melting and the transition to a glass phase appear as a consequence of the interplay between the peculiar vortex-vortex interaction and the pinning mechanism.[3–7] Investigations of the effect of pinning on the vortex lattice as well as on vortex motion[8–11] have shown that the flux-flow behavior can be divided into two distinct regimes: elastic flow, where disorder is weak and the vortex structure essentially moves as a whole, and plastic flow with strong disorder, where the vortex lattice can be torn. The onset of vortex motion in the two regimes can differ substantially in that for plastic flow, vortices can flow in filaments or channels with the rest of the structure remaining pinned.[12,13]

A model for vortex flow in the form of filaments and channels has been proposed recently[14–16] for interpreting experimental results of studies concerning the tearing of the vortex lattice[12] and the current induced transition from plastic to elastic vortex flow.[17] Time integration of the equation of motion as well as Monte Carlo techniques were applied to simulate filamentary flow of vortices and the resulting current-voltage ($IV$) characteristics. Furthermore, discontinuities in $IV$ curves of $2H$-$NbSe_2$ have been observed,[18] which were tentatively ascribed to vortex flow in channels. The channel flow state was found to be metastable and subject to strong history effects. Recently, Matsuda *et al.*[19] showed motion picture recordings of flowing vortices, where depinning processes of single-row vortex structures and subsequent filamentary and channel motion can clearly be seen.

In this paper we report clear evidence for filamentary and channel-vortex flow, which is found in multiple voltage jumps in the $IV$ characteristics of Pb/(14 at.%)In superconducting films in magnetic fields much smaller than the critical field $B_{c2}$ of the superconducting–normal-state transition. The $IV$ curves and thus, the channel flow pattern, are found reproducible even after heating the sample above $T_c$ and recooling. The dependence of the jumps on magnetic field and temperature reveals that the channels or filaments remain constant in size upon small changes of the field, but become unstable with increasing temperature. The $IV$ characteristics exhibit a counterclockwise hysteresis that diminishes as the field is increased and eventually changes into a bistable behavior. With increasing magnetic field more and more channels and filaments are opened up joining into larger streams, until the state of massive vortex motion, i.e., free flux flow is reached. Our results are in good agreement with the predictions of the model of filamentary vortex flow.[16] In particular, the approximately parabolic magnetic field dependence of the threshold depinning force is a fingerprint of channel flow.

Superconducting films of Pb with nominally 14 at.% In were fabricated by evaporation on glass substrates. The sample size is $6\times 6$ mm$^2$ with film thicknesses $d$ ranging from 60 to 300 nm, as determined using atomic-force microscopy (AFM). The superconducting transition in zero field is at $T_c=7.2$ K. For transport experiments, Au leads were either pressed directly against the sample surface or onto pre-evaporated Au contacts. Both methods yielded very similar results. Current-voltage measurements were performed with standard four terminal configuration using dc currents up to 4 A. Experiments were carried out at low temperatures ($2.1\ \mathrm{K}<T<T_c=7.2\ \mathrm{K}$) and low magnetic fields ($0<B<0.5$ T) using a split-coil magnet in combination with a He-bath cryostat. The measurements were performed mainly with the field perpendicular to the film, while the current flowed along the film. Different geometries with the field parallel to the film and the current perpendicular and parallel to the field were also tested.

Although measurements were carried out on several films with different thickness and In composition, here we give values of fundamental parameters for the two samples presented below. The AFM images show that the surface of the films is clustered with an average cluster size of about 50 to 100 nm, thus we take 50 nm as the upper bound for the electronic mean free path $l$. Using this value and the Ginzburg-Landau coherence length of pure Pb $\xi(l=\infty)\simeq 500$ nm (Ref. 20) we estimate $\xi\simeq 150$ nm for our

 

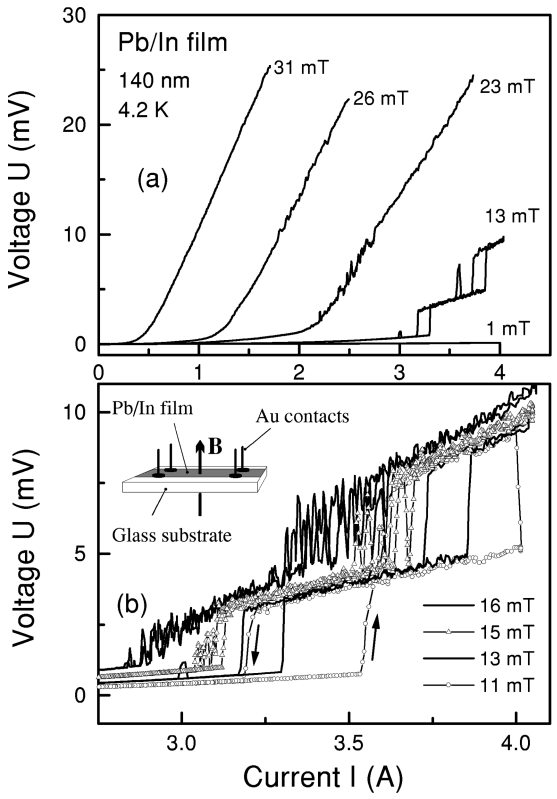


FIG. 1. (a) Current-voltage ($IV$) characteristics of a 140-nm-thick Pb/In sample measured at 4.2 K for different magnetic fields perpendicular to the film. (b) Enlarged view of the $IV$ curves in the jump region. The inset shows a sketch of the sample and contacts for standard four-point transport measurements.

samples.[21] From resistance measurements as a function of temperature at different magnetic fields we obtain $B_{c2}(T=0)\approx 150$ mT extrapolated to zero temperature. Using the critical field for pure Pb [$B_{c,th}(T=0)=80$ mT (Ref. 22)] this gives a $\kappa$ value of around 1.4. Accordingly, the penetration depth $\lambda$ is of the order of 200 nm and the effective penetration depth $\Lambda=2\lambda^2/d\approx 500$ nm. With an average intervortex spacing of $a_0=\sqrt{\phi_0/B}\approx 200$ nm for $B=50$ mT and assuming that the pinning range is $R_p\approx\xi$, we obtain that $R_p<a_0<\Lambda$.

Representative $IV$ characteristics of a 140 nm thick Pb/In sample for different magnetic fields are shown in Fig. 1(a). Data were taken at 4.2 K with the field perpendicular to the film, as shown schematically in the inset to Fig. 1(b). For magnetic fields 23 mT$<B<B_{c2}=80$ mT we observe the characteristic behavior of a type-II superconductor: At low currents the transport is almost dissipationless due to vortex pinning, whereas above a critical current for vortex depinning massive flux flow sets in and the voltage drop across the sample rises linearly with the transport current. With increasing magnetic field $B$ the dissipation onset shifts to lower currents and the differential resistance $\rho_f$ in the dissipation regime follows the simple relationship $\rho_f/\rho_n=B/B_{c2}$, where $\rho_n$ is the normal-state resistance, as expected for free-flux flow.[23]

A striking behavior that cannot be explained within the Bardeen-Stephen flux flow model[23] is observed at low fields ($B<16$ mT), where the $IV$ curves exhibit abrupt voltage jumps. Figure 1(b) shows this part of the $IV$ characteristics in more detail. Succeeding each jump, a linear dissipation region can be seen, the differential resistance being approximately independent of magnetic field. For larger fields, the jumps become smaller and shift towards lower current values. In the jump region, the curves show a large counterclockwise hysteresis upon cycling the current up and back down. It becomes narrower as the magnetic field increases and eventually changes into bistable behavior. These features are highly reproducible with the jumps occurring at the same currents even after heating the sample above $T_c$. Due to thermal activation of vortices, there is a small nonlinear dissipation rise even before the first jump occurred in the $IV$ curves. In contrast, at vanishing fields no kind of dissipation was detected.

Measurements with the field parallel to the film surface were performed to rule out possible contact resistance effects. The $IV$ curves were taken with the current perpendicular and parallel to the field. In the perpendicular case, data exhibited voltage jumps within an overall lower dissipation level. With the current parallel to the field, however, very low dissipation and no jumps were observed. This is a consequence of the vanishing Lorentz force for this configuration and confirms that the jumps arise from vortex flow under a transport current.

We interpret the features observed in the $IV$ curves at low magnetic fields in terms of the motion of vortices in the form of filaments or channels driven by the Lorentz force arising from a transport current. As pointed out in Ref. 16, multiple voltage jumps followed by linear dissipation regions with increasing slope are the signature of filamentary vortex motion. When the shear modulus $C_{66}$ of the vortex lattice is small compared to its compression modulus $C_{11}$, the tearing of the vortex structure is favored over a distortion of the lattice associated with the onset of massive flux flow. Since the effective penetration depth $\Lambda$ is larger than both the sample thickness $d$ and the intervortex distance $a_0$, our samples exhibit two-dimensional (2D) behavior, which means that $C_{66}/C_{11}\ll 1$.[16] A sudden dissipation increase seen as a voltage jump in the $IV$ characteristic is thus associated with the depinning of a filament or channel of vortices. Upon increasing the current, the dissipation rises linearly, indicating that the number of moving vortices is constant. When the next channel is set in motion, an additional jump appears in the $IV$ curve. With increasing magnetic field, the filaments depin at lower currents, since the Lorentz force is larger. The hysteresis arises because on the downward current ramp the filament flow is stable down to a point below the initial depinning. At larger magnetic fields the hysteretic behavior transforms into a bistable one with voltage jumps at fixed currents, in which case a filament is depinned, then stopped, then depinned again and so forth.

The dependence of the voltage jumps on temperature indicates that filament formation becomes increasingly unstable while approaching $T_c$. Figure 2 shows $IV$ curves taken at constant perpendicular magnetic field and for temperatures between 3.7 and 6.6 K. The significant difference between curves measured below and above 4.2 K is due to the fact that, in the former case, the sample is immersed in liquid He and heat removal is very efficient. Above 4.2 K, the resistance values reached after the jumps are approxi-

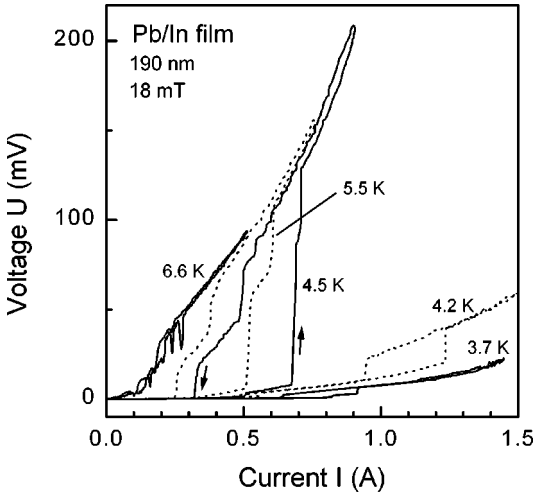


FIG. 2. Current-voltage characteristics of a 190-nm-thick Pb/In sample taken at different temperatures with a perpendicular magnetic field of 18 mT. Arrows indicate the direction of the current change.

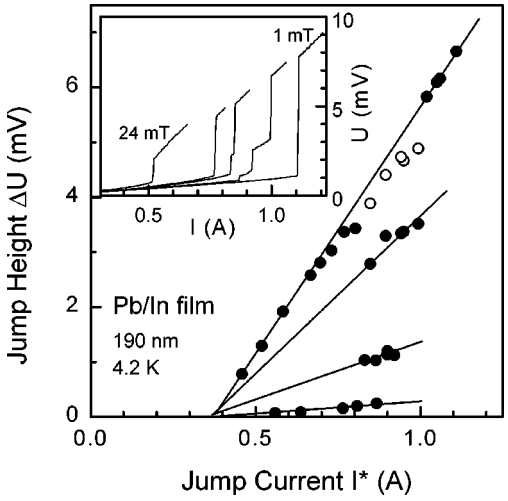


FIG. 3. Voltage jump height $\Delta U$ versus the current $I^*$ at which the jumps occur, as determined from current-voltage characteristics of a 190-nm-thick Pb/In sample with perpendicular field at 4.2 K. Open circles correspond to the sum of the individual jump heights for the $IV$ curves displaying multiple steps. Solid lines represent fits to the data using a linear relation. The inset shows original $IV$ curves (only upward current ramps).

mately that of the normal conducting state and the current-voltage curves bend slightly upwards due to sample heating. In addition, the downward current ramp clearly displays a series of small steps before the zero-dissipation state is reestablished signalizing the breakup of filaments into smaller ones.

The multistep behavior at higher temperatures (see Fig. 2) can be explained by considering the temperature variation of the shear modulus $C_{66}$. It determines how easily a filament can be separated from the rest of the vortex lattice, the latter remaining pinned. Taking into account the temperature dependence of the penetration depth $\lambda$ (Ref. 21) the shear modulus can be written as[8]

$$C_{66}=\frac{B\phi_0}{16\pi\mu_0\lambda_0^2}\left[1-\left(\frac{T}{T_c}\right)^4\right], \qquad (1)$$

where $\phi_0$ is the magnetic-flux quantum, $\mu_0$ is the vacuum permeability, and $\lambda_0=\lambda(T=0)$. Thus, $C_{66}$ drops with increasing temperature. This implies that smaller fractions of the total number of vortices in the sample are torn off more easily giving rise to the multistep features in the $IV$ curves of Fig. 2.

A remarkable result concerns the differential resistance of the $IV$ characteristics between two successive jumps, which is essentially constant for varying magnetic field. This behavior, which is not expected for massive flux flow, is an indication that the number of moving fluxoids in the respective channel remains unchanged, even when the magnetic field is increased. This can be confirmed by examining the jump heights $\Delta U$. Since the dissipation voltage arising from the motion of a single vortex is proportional to the vortex speed, we obtain the total voltage $U_{\rm diss}\propto N_{\rm v} I\phi_0$, where $N_{\rm v}$ is the number of moving vortices in the channel, $I$ the transport current and $\phi_0$ the magnetic-flux quantum. The jump heights for different magnetic fields are plotted in Fig. 3 against the currents $I^*$ at which the jumps occurred (the original $IV$ curves are shown in the inset). The data exhibit a linear relationship between $\Delta U$ and $I^*$, from which we conclude that for channel flow $N_{\rm v}$ is a constant.

Furthermore, at some magnetic fields we observe the splitting of a voltage jump into smaller portions which later join back together. The heights of these portions also vary linearly with current but have different slopes; added together they roughly fit the data of the main jump (open circles in Fig. 3). Here, the large voltage jump at lower ($<5$ mT) and higher ($>10$ mT) magnetic fields is associated with a wide stream of filaments which in the intermediate field region is subdivided into three smaller channels. The extrapolations of the linear dependences of the jump heights to lower currents meet at approximately the same point on the current axis. This is a strong indication of the existence of a critical magnetic field for which the jump heights, independent on the size of the filaments, strictly vanish. Above this critical field the $IV$ curves exhibit a kink at the dissipation onset rather than jumps. Hence, it marks the border between filamentary and free-flux flow. This might be a manifestation of the vortex-vortex interaction becoming stronger with increasing magnetic field, such that at this point the shear modulus $C_{66}$ [see Eq. (1)] exceeds a critical value above which filament formation is not favorable.

Further insight into the vortex depinning process is obtained by examining the jump currents $I^*$ multiplied by the respective magnetic induction $B$, the product being a measure of the threshold depinning force $F_{dep}$ exerted on the vortex lattice. As shown in Fig. 4, with increasing magnetic field $F_{dep}(B)$ rises from zero and displays a maximum shortly before the voltage jumps disappear. This behavior is well described by a parabolic relationship (solid curve in Fig. 4). Similar results have been obtained for the pinning force density in polycrystalline NbN films.[24] As pointed out in Ref. 15, this field dependence of the threshold depinning force can be explained in terms of vortex channels flowing past regions of vortices trapped by pinning centers. This is the case for strong pinning where the depinning force is de-

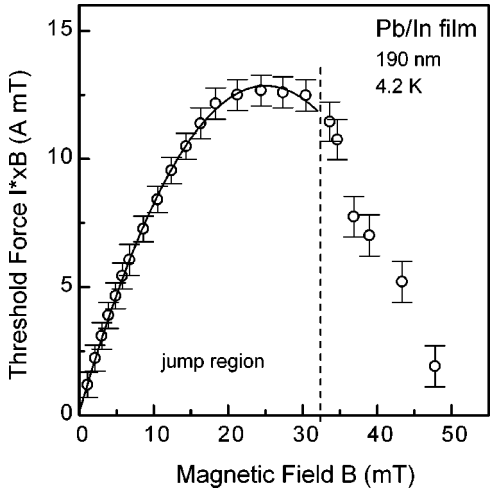


FIG. 4. Threshold depinning force $F_{dep} \propto I^*B$ as a function of the external magnetic field $B$ for a 190-nm-thick Pb/In sample at 4.2 K. The solid line represents a fit to the data below 30 mT using a parabolic relation.

termined mainly by vortex-vortex interactions and largely independent of the pinning potential depth $A_p$. Moreover, with increasing field $F_{dep}$ grows in proportion to the shear modulus $C_{66}$, which means that above a critical $B$ value channel flow is superseded by massive vortex motion.

In conclusion, we have obtained direct evidence for filamentary and channel-vortex flow in low-$T_c$ superconducting films from voltage jumps in $IV$ characteristics at low magnetic fields compared to $B_{c2}$. In the filamentary-flow regime, $IV$ curves exhibit a pronounced counterclockwise hysteresis which transforms into bistable behavior for magnetic fields close to that of the onset of free-flux flow. At low temperatures compared to $T_c$, channel flow is found to proceed with a constant number of vortices per filament upon small changes in the magnetic field. At higher temperatures, the flow pattern becomes unstable resulting in a larger number of smaller channels that flow individually. Both the magnetic field dependence of the depinning force and the existence of a critical field beyond which filamentary motion is not observed are manifestations of the pinning mechanism being governed by vortex-vortex interactions. In this way, we have provided new results of the vortex dynamics in low-$T_c$ superconducting thin films, for which a distortion of the vortex lattice in form of filaments is favored against massive flux flow by intervortex interactions.

We thank T. Wehnert for the AFM measurements, D. Domínguez for helpful discussions, and E. H. Brandt for careful reading of the manuscript.

[1] S. T. Chui and B. Tanatar, Phys. Rev. Lett. **74**, 458 (1995); Y. P. Li *et al.*, *ibid.* **67**, 1630 (1991).
[2] G. Grüner, Rev. Mod. Phys. **60**, 1129 (1988).
[3] D. S. Fisher, M. P. A. Fisher, and D. A. Huse, Phys. Rev. B **43**, 130 (1991).
[4] W. K. Kwok, J. Fendrich, S. Fleshler, U. Welp, J. Downey, and G. W. Crabtree, Phys. Rev. Lett. **72**, 1092 (1994).
[5] R. H. Koch, V. Foglietti, W. J. Gallagher, G. Koren, A. Gupta, and M. P. A. Fisher, Phys. Rev. Lett. **63**, 1511 (1989).
[6] H. Safar, P. L. Gammel, D. J. Bishop, D. B. Mitzi, and A. Kapitulnik, Phys. Rev. Lett. **68**, 2672 (1992).
[7] H. Safar, P. L. Gammel, D. A. Huse, D. J. Bishop, J. P. Rice, and D. M. Ginsberg, Phys. Rev. Lett. **69**, 824 (1992).
[8] A. I. Larkin and Yu. N. Ovchinnikov, J. Low Temp. Phys. **34**, 409 (1979).
[9] R. Wördenweber, P. H. Kes, and C. C. Tsuei, Phys. Rev. B **33**, 3172 (1986).
[10] P. Berghuis and P. H. Kes, Phys. Rev. B **47**, 262 (1993).
[11] S. Bhattacharya and M. J. Higgins, Phys. Rev. B **49**, 10 005 (1994).
[12] S. Bhattacharya and M. J. Higgins, Phys. Rev. B **52**, 64 (1995).
[13] G. D'Anna, P. L. Gammel, H. Safar, G. B. Alers, D. J. Bishop, J. Giapintzakis, and D. M. Ginsberg, Phys. Rev. Lett. **75**, 3521 (1995).
[14] E. H. Brandt, J. Low Temp. Phys. **53**, 41 (1983): **53**, 71 (1983).
[15] H. J. Jensen, Y. Brechet, and A. Brass, J. Low Temp. Phys. **74**, 293 (1989).
[16] N. Grønbech-Jensen, A. R. Bishop, and D. Domínguez, Phys. Rev. Lett. **76**, 2985 (1996).
[17] M. C. Hellerqvist, D. Ephron, W. R. White, M. R. Beasley, and A. Kapitulnik, Phys. Rev. Lett. **76**, 4022 (1996).
[18] W. Henderson E. Y. Andrei, M. J. Higgins, and S. Bhattacharya, Phys. Rev. Lett. **77**, 2077 (1996).
[19] T. Matsuda, K. Harada, H. Kasai, O. Kamimura, and A. Tonomura, Science **271**, 1393 (1996); Ch.-H. Sow, K. Harada, A. Tonomura, G. Crabtree, and D. Grier, Phys. Rev. Lett. **80**, 2693 (1998).
[20] J. J. Hauser, Phys. Rev. B **10**, 2792 (1974).
[21] W. Buckel, *Supraleitung* (VCH, Weinheim, 1994), p. 157.
[22] W. Buckel, *Supraleitung* (Ref. 21), p. 112.
[23] J. Bardeen and M. J. Stephen, Phys. Rev. **140**, A1197 (1965).
[24] A. Pruymboom, W. H. B. Hoondert, H. W. Zandbergen, and P. H. Kes, Jpn. J. Appl. Phys., Suppl. **26-3**, 1529 (1987).